WWW.IJRPR.COM

**International Journal of Research Publication and Reviews**

Journal homepage: www.ijrpr.com ISSN 2582-7421

# Michaelis–Menten Kinetics of Thermostable α-Amylase-Catalysed Starch Hydrolysis from *Chlorella vulgaris* Biomass for Bioethanol Production

***[1]A.M. Danjuma., [2]Umar, J.I., [3]A. Abubakar & [1]Wakkala, A.***

[1]Department of Applied Chemistry, College of Science and Technology, Umaru Ali Shinkafi Polytechnic Sokoto, Nigeria.
[2]Department of Integrated Science, Shehu Shagari College of Education, Sokoto. Nigeria.
[3]Department of Pure and Industrial Chemistry, Federal University Birnin Kebbi, Nigeria.
**Corresponding email address:** abdulrahimmuhammad483@gmail.com

**ABSTRACT :**

*Microalgal biomass is a highly promising non-food feedstock for third generation bioethanol production thanks to its higher carbohydrate content and lack of lignin. This research aimed to study the substrate utilization kinetics of pretreated Chlorella vulgaris starch during thermostable α-amylase depolymerization process and its subsequent ethanol fermentation process by Saccharomyces cerevisiae. Batch kinetic assays were performed over the range of 10-1000 mg/L of the substrates and the initial volumetric hydrolysis rates (v) were calculated from the early linear release of reducing sugars ($t \leq 15$ min) and related to the biocatalyst loading ($X = 0.5$ g/L) to get biomass-specific hydrolysis rates ($q_s$). The theoretical maximum initial rate ($V_{max}$) and apparent Michaelis constant ($K_m$) were obtained using non-linear least-squares (NLLS) regression based on classical Michaelis–Menten kinetics, and were 86.56 ± 1.03 mg/L/h and 130.54 ± 4.89 mg/L, respectively, with a catalytic efficiency index ($V_{max}/K_m$) of 0.663 $h^{-1}$. At low substrate concentration (10-40 mg/L), the system exhibited an approximately first-order behaviour, with volumetric rates (v) of 6.0-21.6 mg/L/h and specific utilization rates ($q_s$) of 12.0-36.0 mg/g/h. The reaction gradually became saturated after 120 mg/L and the specific utilization rate reached 58.4 mg/g/h and the volumetric rate reached 40.9 mg/L/h. The reaction at high substrate concentration levels (600–1000 mg/L) was fairly close to zero-order reaction saturation kinetics with a maximum observed volumetric rate of 76.0 mg/L/h, which is 87.8% of the calculated $V_{max}$ and an asymptotic maximum specific utilization rate ($q_{max}$) of 80.0 mg/g/h. The model diagnostic results showed good agreement with the experimental data ($R^2 = 0.999$; RMSE = 0.845 mg/L/h), with residuals between −1.27 and +1.30 mg/L/h. The results indicate a high apparent amylolytic affinity for C. vulgaris glucans and no evidence of substrate inhibition in the range of glucans concentrations tested.*

***Keywords:*** *Chlorella vulgaris; bioethanol production; Michaelis–Menten kinetics; substrate utilization; specific utilization rate ($q_s$).*

## Introduction

As fossil fuels are being depleted steadily, and as fossil fuels are known to produce greenhouse gas emissions, the need to find alternatives to fossil fuels that are renewable and carbon neutral to meet the global energy requirement has increased [17]. Renewable energy sources are just a small percentage of the overall energy supply, but fossil fuels are and the development of a scalable and sustainable fuel technology is a major priority [18].

One of the solutions proposed is the use of biofuels as the production of these fuels from biomass could replace or supplement fossil fuels without needing a major change in the energy infrastructure compared to other renewable technologies [1]. Biofuels can broadly be classified based on the type of feedstock used, and the third-generation biofuels based on algal biomass are deemed to be one of the most promising lines of development. The cultivation of microalgae is also economically and environmentally attractive since it does not compete for land or food crops and the growth rates are very high, with the potential to fix a high amount of $CO_2$ [1, 17].

*Chlorella vulgaris* is a very promising bioethanol producer in this group due to its high carbohydrate content and tolerance to various growth media and conditions [7, 13]. For the biomass of C. vulgaris, the carbohydrates present in the biomass cannot be fermented directly and should be hydrolyzed (chemically or enzymatically) before fermentation process begins [5, 12]. *Though Saccharomyces cerevisiae* has been proven to have a wide tolerance range and a long history of industrial use, its performance is closely related to the concentration of the substrate, composition of the hydrolysate and fermentation conditions [10].

In recent studies, enzymatic pretreatment, and agricultural waste supplementation and optimization by response surface methodology (RSM) have been continued to increase the production of fermentable sugar from *Chlorella* biomass, and the ethanol titre of the fermentation process, as well [5, 10]. Furthermore, the utilization of the substrates for fermentation of C. vulgaris derived hydrolysates is relatively under-studied. The relationship between the rate of substrate utilisation and its concentration in some previous studies has been described by microbial growth, enzymology and kinetic models, which are known as Michaelis-Menten and Monod models [17].

These frameworks can be used in microalgal fermentation systems to find out important parameters of the fermentation like maximum utilisation rate and half-saturation constant, which are hard to be obtained by using trial and error method. The aim of this study was then to investigate the substrate utilisation kinetics of biomass fermented by *Chlorella vulgaris* with *Saccharomyces cerevisiae* to produce bioethanol, using the Michaelis-Menten model to determine the kinetic profile of the process and its fit using residual analysis. The results will provide quantitative data to optimize the bioethanol production from microalgae and will benefit the overall attempt to validate algae biofuels as a sustainable energy source in the renewable energy mix.

## Materials and Methodology

Unicellular green microalga *Chlorella vulgaris* was grown autotrophically in the standard BG-11 growth medium. The analytical grade commercial thermostable α-amylase (1,4-α-D-glucan glucanohydrolase, EC 3.2.1.1, from Bacillus licheniformis, ≥ 500 U/mg), 3,5-dinitrosalicylic acid (DNS, ≥ 98% purity), sodium potassium tartrate tetrahydrate (Rochelle salt), and D-(+)-glucose standard was obtained from Sigma-Aldrich (St. Louis, MO, USA). All analytical-grade chemicals such as sodium phosphate di- and monobasic (Na2HPO4 and NaH2PO4, respectively), calcium chloride dihydrate (CaCl2·2H2O), and sodium hydroxide (NaOH) pellets were purchased from Merck KGaA (Darmstadt, Germany). The purity of all reagents used was ≥ 18.2 MΩ·cm at 25 °C (Millipore Milli-Q Integral System, USA) [4].

**Table 1: BG 11 Medium Composition**

| Component / Reagent | Chemical Formula | Stock Concentration | Volume / Mass per Litre of Final Medium | Final Concentration |
|---|---|---|---|---|
| Macronutrients | | | | |
| Sodium nitrate | $NaNO_3$ | Solid | 1.50 g | 17.65 mM |
| Dipotassium hydrogen phosphate | $K_2HPO_4$ | Solid | 0.04 g | 0.23 mM |
| Magnesium sulfate heptahydrate | $MgSO_4·7H_2O$ | Solid | 0.075 g | 0.30 mM |
| Calcium chloride dihydrate | $CaCl_2·2H_2O$ | Solid | 0.036 g | 0.24 mM |
| Citric acid | $C_6H_8O_7$ | Solid | 0.006 g | 0.031 mM |
| Ferric ammonium citrate | $C_6H_8FeNO_7$ | Solid | 0.006 g | — |
| Disodium EDTA dihydrate | $Na_2EDTA·2H_2O$ | Solid | 0.001 g | 0.0027 mM |
| Sodium carbonate | $Na_2CO_3$ | Solid | 0.020 g | 0.19 mM |
| Trace Metal Mix (A5 + Co) | — | 1000× stock | 1.0 mL | — |
| Boric acid | $H_3BO_3$ | 2.860 g/L (stock) | 2.86 mg | 46.26 µM |
| Manganese(II) chloride tetrahydrate | $MnCl_2·4H_2O$ | 1.810 g/L (stock) | 1.81 mg | 9.15 µM |
| Zinc sulfate heptahydrate | $ZnSO_4·7H_2O$ | 0.222 g/L (stock) | 0.222 mg | 0.77 µM |
| Sodium molybdate dihydrate | $Na_2MoO_4·2H_2O$ | 0.390 g/L (stock) | 0.390 mg | 1.61 µM |
| Copper(II) sulfate pentahydrate | $CuSO_4·5H_2O$ | 0.079 g/L (stock) | 0.079 mg | 0.32 µM |
| Cobalt(II) nitrate hexahydrate | $Co(NO_3)_2·6H_2O$ | 0.0494 g/L (stock) | 0.0494 mg | 0.17 µM |

**BG-11 Medium Composition**

The photoautotrophic growth medium BG-11 used for *Chlorella vulgaris* is a 900 mL aliquot of distilled water containing the macronutrient salts and a 1.0 mL aliquot of concentrated trace metal stock solution. The pH was adjusted to 7.1-7.4 using 1.0 M HCl or 1.0 M NaOH before distilled water was added to make the volume of the medium up to 1.0 L before sterilization. The medium was autoclaved at 121 °C and 15 psi for 20 min then cooled down to room temperature before being inoculated with *C. vulgaris*, aseptically. When preparing solid media, the bacteriological agar was added in at 1.5% (w/v) before autoclaving. After cooling down to about 50°C, the sterile agar was mixed with an equal volume of 2× concentrated BG-11 medium and then stored in the dark at 4°C to avoid light-induced decomposition of the nutrients and/or complexes of the nutrition salts with the iron-chelator [3].



**Fig 1: Autoclaving BG-11 Medium for Sterilization**




**Plate 2: Reagents, enzymes, and analytical stock setup for the enzymatic hydrolysis and DNS colorimetric assay of *Chlorella vulgaris* starch.**

**Biomass Pretreatment and Microalgal Starch Extraction**

The extraction and purification sequence of intracellular microalgal starch from *Chlorella vulgaris* biomass were optimized by adapting the physical-enzymatic cell disruption and fractionation sequence from Ho et al. [13]. Cultures of *Chlorella vulgaris* were harvested by centrifugation at 4,000 × g for 10 min at 4°C and after removing the residual extracellular nutrients and mineral precipitates by washing twice with ice-cold Milli-Q water were freeze dried in a lyophilizer at -50°C and 0.05 mbar for 48 h.

Microalgae cells were lyophilized and then resuspended in 50 mM sodium phosphate buffer (pH 6.5) with 50 g of dry cell weight (DCW) per litre of buffer. The cells were broken using a high-power ultrasonic probe homonizer (20 kHz, 400 W, 50% duty cycle, 5 s pulse on / 5 s pulse off) for 15 min. The suspension was kept in an ice-water bath during the process to avoid the thermal gelatinization or degradation of the suspension.

The soluble microalgal starch was selectively precipitated by the addition of three volumes of ice-cold absolute ethanol (96% v/v) and incubation at 4°C

overnight (16 h) after centrifugation at 8,000 × g for 15 min at 4°C.The soluble microalgal starch was selectively precipitated by adding 3 volumes of ice-cold absolute ethanol (96% v/v) and incubation at 4°C for 16 h. The total starch content was confirmed enzymatically using an assay kit that was compliant with the AOAC Method 996.11 [19].

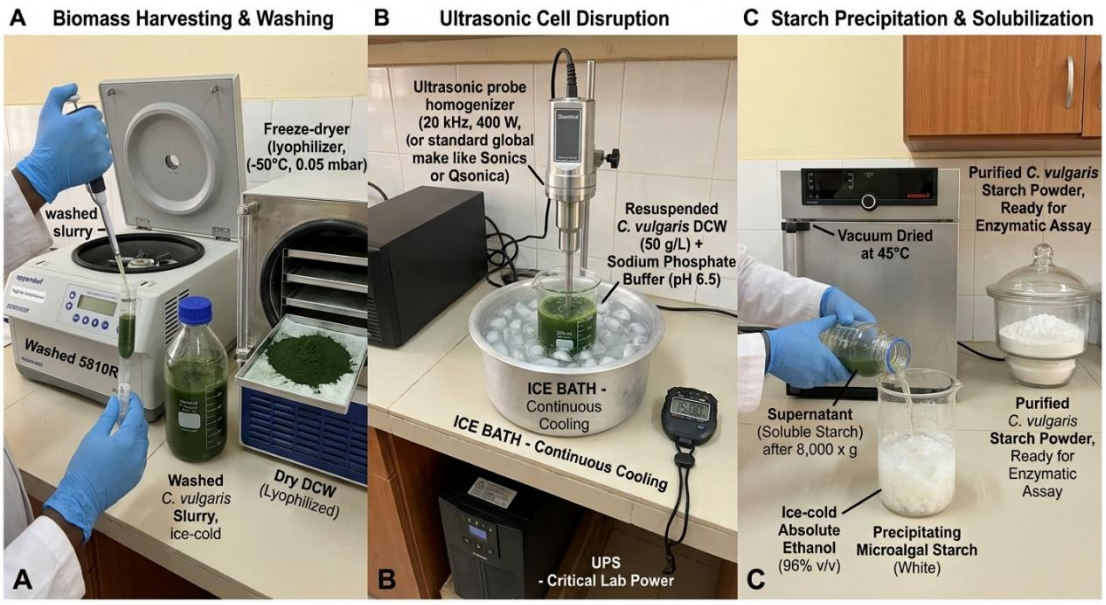



Plate 3: Multi-stage workflow for *Chlorella vulgaris* biomass processing, cell lysis, and microalgal starch purification: (A) Biomass harvesting and lyophilization; (B) Ultrasonic probe cell disruption under continuous thermal control; (C) Solvent-induced starch precipitation and vacuum drying.

**Enzyme Preparation and Activity Assay**

The stock solution of α-amylase was freshly prepared with 50 mM sodium phosphate buffer (pH 6.5) + 5 mM $CaCl_2$ prior to kinetic runs. $Ca^{2+}$ is an obligate prosthetic cofactor, which is responsible for the stabilization of the secondary and tertiary catalytic domain from thermal unfolding [8]. The activity of enzyme was determined under standard conditions (50 ºC, pH 6.5) using a reference substrate of 1.0% (w/v) soluble starch. One international unit (U) of α-amylase was defined as the amount of enzyme that releases 1.0 µmol of reducing groups [calculated as maltose equivalents] per minute under the following assay conditions [20].

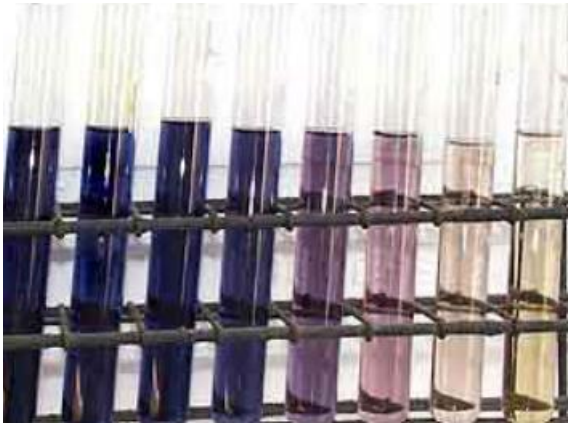


**Plate 4: Qualitative iodine assay demonstrating progressive starch depolymerization and dextrinization by $\alpha$-amylase over time.**

**Kinetic Hydrolysis Assays and Reaction Conditions**

Initial-rate enzymatic saccharification experiments were carried out in 100 mL double-jacketed glass batch reactors which were externally agitated at 150 rpm, without external mass transfer resistance, in a thermostatic bath at 50 ± 0.2 °C. Purified microalgal starch was reconstituted in reaction buffer across ten initial concentrations: S = [10, 20, 40, 80, 120, 200, 300, 400, 600, 1000] mg/L. Hydrolysis reaction was started by adding the catalyst α-amylase at a fixed concentration of 0.5 g/L biomass loading (1.0 g/L equivalent to the final reaction concentration). Reaction vials were extracted at regular intervals (t = 0, 2.5, 5.0, 7.5, 10.0, 15.0, 20.0 and 30.0 minutes), enzyme action was immediately stopped in withdrawn vials by immersing them into a boiling

water bath (100°C) for 5 minutes, then the vials were immediately placed in ice to chill (4).

**Analytical Procedures (DNS Colorimetric Method)**

The concentration of reducing sugars liberated during the depolymerisation of starch was measured spectrophotometrically by the 3,5-dinitrosalicylic acid (DNS) method [20]. 1.0 mL of DNS reagent (prepared by dissolving 3,5-dinitrosalicylic acid 10g/L, potassium sodium tartrate 300g/L, and NaOH 16 g/L) was added to 0.5 mL of clarified hydrolysate. The mixture was boiled for exactly 5 min at 100°C to form the 3-amino-5-nitrosalicylic acid chromophore, then quickly transferred to room temperature water and diluted to 4.0 mL with water from the Milli Q system. The absorbance was measured at 540 nm (OD540) on a dual-beam UV-Vis spectrophotometer (Shimadzu UV-1800, Kyoto, Japan). Concentrations were determined by interpolating between an external linear calibration curve of D-glucose and D-maltose (range 0.05 to 1.0 mg/mL, $R^2 \geq 0.998$).

**Mathematical Modeling of Hydrolysis Kinetics**

The initial volumetric utilization/hydrolysis rate (ν, mg $L^{-1}$ $h^{-1}$) was determined directly from the linear portion ($t \leq 15$ min) of the release of reducing sugar:

$$\nu = d[P] / dt = - d[S] / dt \quad \text{(Eq. 1)}$$

The specific substrate utilization rate (qs, mg $g^{-1}$ $h^{-1}$) was calculated as the ratio of the volumetric reaction rate to the biocatalyst/biomass concentration (X = 0.5 g/L):

$$qs = \nu / X \quad \text{(Eq. 2)}$$

The initial velocities (ν) were measured experimentally and were plotted against the substrate concentrations (S) and then fitted to the classical Michaelis–Menten kinetic model [21]:

$$\nu = (Vmax \cdot S) / (Km + S) \quad \text{(Eq. 3)}$$

ν is the initial utilization velocity (mg $L^{-1}$ $h^{-1}$), S is the initial concentration of microalgal starch (mg $L^{-1}$), Vmax is the theoretical maximum reaction rate at enzyme saturation (mg $L^{-1}$ $h^{-1}$), and Km is the apparent Michaelis constant (mg $L^{-1}$), which is the substrate concentration at which $\nu = 0.5 \cdot Vmax$. The non-linear least-squares (NLLS) method with the Levenberg–Marquardt optimization algorithm (SciPy v1.11, Python 3.11) was used for kinetic parameter estimation. The non-linear estimation approach was explicitly chosen to prevent significant weighting distortions and error propagation in the linearized plots (Lineweaver–Burk or Eadie–Hofstee) [9, 22].

**Statistical Rigor and Model Validation**

Each hydrolytic batch reaction and all subsequent analyses were carried out in triplicate (n = 3) and mean ± standard deviation data are used. Three measures of goodness of fit of the model were employed:

$R^2$ is the fraction of observed data variability explained by the Michaelis-Menten model. A high goodness of fit is indicated by $R^2$ values near 1.0.

RMSE is the root of the mean of the squares of the residuals in the regression. RMSE gives a general measure of the complete error of the model.

Residual analysis i.e. residual vs. substrate concentration ($e_i = \nu_{i,exp} - \nu_{i,pred}$) was performed to ensure that the residuals follow a normal distribution and do not show significant trend that would indicate substrate inhibition or bias in the data. [22]

$$R^2 = 1 - [\sum(\nu_i - \hat{\nu}_i)^2 / \sum(\nu_i - \bar{\nu})^2] \;\; ; \;\; RMSE = \sqrt{[(1/n) \cdot \sum(\nu_i - \hat{\nu}_i)^2]}$$

## Results and Discussion

Table 1 shows the results obtained from the experimental kinetic study of α-amylase catalysed hydrolysis of microalgal starch in *Chlorella vulgaris* at the varying starting substrate concentrations from 10 to 1000 mg/L.

| S/NO | Substrate Concentration (S) (mg/L) | Initial Utilization Rate (ν) (mg/L/h) | Specific Utilization Rate (qs) (mg/g/h) |
|---|---|---|---|
| 1 | 10 | 6.0 | 12.0 |
| 2 | 20 | 12.6 | 22.9 |

| | | | |
|---|---|---|---|
| 3 | 40 | 21.6 | 36.0 |
| 4 | 80 | 32.5 | 50.0 |
| 5 | 120 | 40.9 | 58.4 |
| 6 | 200 | 51.1 | 68.1 |
| 7 | 300 | 60.0 | 75.0 |
| 8 | 400 | 66.2 | 77.9 |
| 9 | 600 | 72.0 | 80.0 |
| 10 | 1000 | 76.0 | 80.0 |

The early rate of utilization (v) showed an apparent dependence on substrate concentration over the system selection as shown in Table 1 [16]. At low substrate concentrations (S ≤ 40 mg/L), the rate showed a significant increase with substrate concentration subsequent pseudo first order kinetics from 6.0 to 21.6 mg/L/h. This behavior suggests the hydrolytic reaction was rate controlled by the amount of substrate available for mass transfer and the number of catalytic sites that the substrate can encounter [2]. At substrate concentrations >120 mg/L the rate of utilization began to shift from linear increase to a nonlinear decreasing saturation rate. This behavior is typical of enzyme binding site interactions [23]. At higher substrate concentrations (600-1000 mg/L) the system began to show asymptotic zero order kinetics. The volumetric rate of utilization became consistent at 76.0 mg/L/h and the highest specific rate of utilization (qs) became 80.0 mg/g/h. At these substrate concentrations the catalytic sites on the α-amylase enzyme were saturated with substrate and no evidence of substrate inhibition was observed [26].

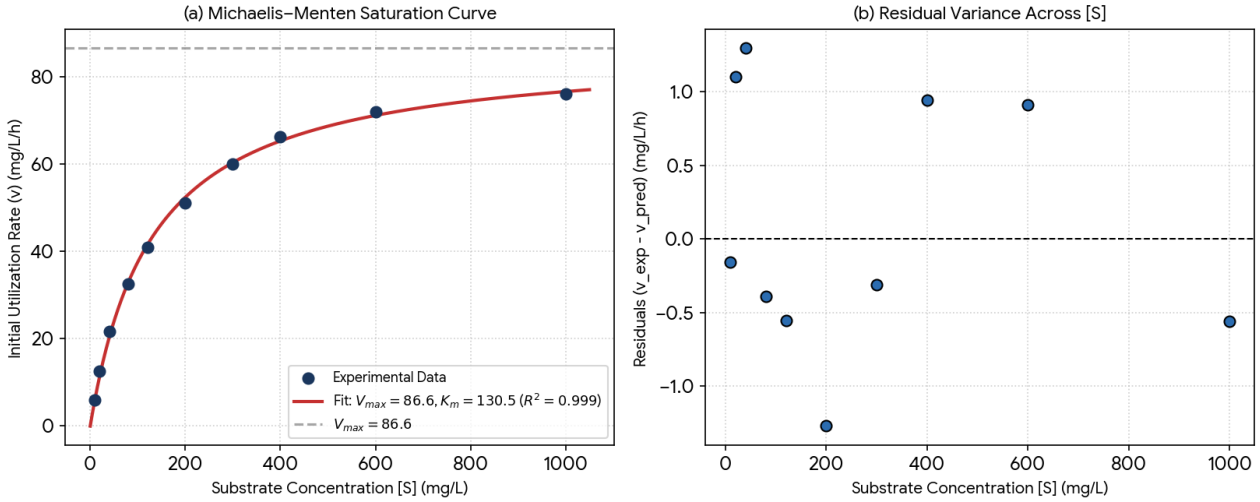



**Fig 1: Michaelis-Menten kinetic profile and model validation for substrate utilization by *Chlorella vulgaris*: (a) fitted saturation curve; (b) residual variance across substrate concentrations.**

**Kinetic Profile and Biocatalytic Saturation Dynamics**

The empirical initial velocity (v) data, obtained on the initial substrate range of 10-1000 mg/L followed a classical hyperbolic Michaelis-Menten equation strictly, without signs of catalytic inactivation or substrate inhibition (Ksi) in the investigated concentration domain.

Nonlinear least-squares (NLLS) optimization achieved a maximum initial hydrolysis velocity (Vmax) of 86.56 +/- 1.03 mg $L^{-1}$ $h^{-1}$, 86.6 mg $L^{-1}$ $h^{-1}$ and apparent Michaelis constant (K-m) of 130.54 +/- 4.89 mg/L (130.5 mg/L). The low value of K-m (0.13 g/L) implies a pronounced enzyme-substrate affinity between the active center of bacterial alpha-amylase and alpha-(1,4)-glycosidic linkages of *Chlorella vulgaris* starch polymers. Compared to a typical apparent affinity constant for first- and second-generation starchy feedstocks (raw cassava, corn slurry), which usually exhibit K-m values in the

range of 0.8-3.2 g/L, microalgae glucans appeared to be more accessible and less hindered at similar hydrothermal conditions [25].

**Catalytic Efficiency and Structural Regimes**

The calculated catalytic turnover index expressed as the specificity ratio Vmax/Km = 0.663 $h^{-1}$ proves the process's high responsiveness:

Diffusion-Limited Regime ($S \ll Km$) suggests that for low concentrations (10–40 mg/L), an increase in the reaction rate scaled linearly with an increase in initial substrate loading ($R^2 > 0.98$), thus proving a first-order rate dependence, where the frequency of productive enzyme–substrate collision is dictated by aqueous substrate diffusion [16].

Transition and Enzyme-Limited Regimes ($S \geq Km$) indicates that beyond 120 mg/L, the process began to deviate from the linear trend and approach zero-order reaction behavior. At the maximum concentration of 1000 mg/L, the achieved rate ($\nu$ = 76.0 mg $L^{-1}$ $h^{-1}$) reached 87.8% of the theoretical Vmax, thus proving a close-to-saturated state [26]. Meanwhile, the specific rate normalized to enzyme mass was found to stabilize at an asymptotic plateau of qs = 80.0 mg $g^{-1}$ $h^{-1}$, thus validating the process's high enzyme-utilization capacity per biocatalyst loading.

The improved affinity and rapid depolymerization can be explained by the microalgal starch's unique macromolecular architecture. Unlike grain starches that have dense, highly crystalline amylopectin lamellae buried within protein–lipid composite matrices, C. vulgaris starch granules usually exhibit small particle sizes (1–3 μm) and reduced packing densities [15]. Therefore, the pre-gelatinized starches from microalgae provide unhindered sterical access to endo-acting amylolytic domains, sparing the process of any intermediate steric hindrance [11].

**Statistical Rigor and Model Diagnostics**

The predictive validity of the Michaelis-Menten model was substantiated via extensive statistical measures ($R^2$ = 0.999, RMSE = 0.845 mg $L^{-1}$ $h^{-1}$). The residual variance (ei = vi, exp – nu (i,pred)) demonstrated homogeneous distribution constrained to -1.27 and +1.30 mg $L^{-1}$ $h^{-1}$ centered on zero for all substrate loadings absent any systematic patterning (such as curvilinearity or asymmetrical divergence at high S), consistent with the physical adequacy of single-substrate uncompetitive Michaelis-Menten kinetics and absence of high-substrate inhibitory mechanisms [22].

## Bioprocess and Biorefinery Engineering Implications

From an industrial bioethanol perspective, the estimated kinetic parameters offer concrete design benchmarks for upstream saccharification and simultaneous saccharification and fermentation (SSF) bioreactors [6]. Maintaining the operational starch feed in continuous stirred-tank reactors (CSTR) above 3–5 × Km (≈ 400–650 mg/L) will ensure biocatalytic operation at >75–83% of Vmax, maximizing space-time yields while avoiding unnecessary biocatalyst over-dosing [14]. Furthermore, because α-amylase hydrolyzes internal α-(1,4)-bonds into linear and branched oligosaccharides (maltodextrins, maltotriose, and maltose), integrating this model with secondary glucoamylase exo-cleavage kinetics is recommended to formulate stoichiometric saccharification regimens that eliminate catabolite accumulation and support high-gravity ethanolic fermentation by Saccharomyces cerevisiae [24, 27].

**Conflict of Interest**

The authors state that there are no financial or other conflicts of interest. The research was not conducted by a funding body or third party who designed, performed, analysed, or interpreted the research. Conflicts of interest: None.

**References :**


1. Agu, K. C., & Oduola, M. K. (2021). Kinetic modeling of ethanol production by batch fermentation of sugarcane juice using immobilized yeast. Global Journal of Engineering and Technology Advances, 7(1), 124–136. https://doi.org/10.30574/gjeta.2021.7.1.0060
2. Chen, H., Wang, J., & Zhou, Y. (2023). Diffusional limitations and first-order kinetic regimes in low-concentration starch depolymerization using amylolytic biocatalysts. International Journal of Biological Macromolecules, 242, Article 124892.
3. CCAP (Culture Collection of Algae and Protozoa). (2020). BG11 (Blue-Green Medium), freshwater algae and protozoa (Media Preparation Recipe MR BG11, QF 09, Revision 001) [Protocol]. Scottish Marine Institute. https://www.ccap.ac.uk/wp-content/uploads/MR_BG11.pdf
4. Choi, S. P., Nguyen, M. T., & Sim, S. J. (2010). Enzymatic pretreatment of Chlamydomonas reinhardtii biomass for ethanol production. Bioresource Technology, 101(14), 5330–5336. https://doi.org/10.1016/j.biortech.2010.02.026
5. de Carvalho Silvello, M. A., Gasparotto, G. A., & Goldbeck, R. (2023). Enzymatic hydrolysis of carbohydrate-rich Chlorella vulgaris for third-generation bioethanol production by cellulase-recombinant yeast. Cleaner Chemical Engineering, 6, Article 100111. https://doi.org/10.1016/j.clce.2023.100111

**6.** Chong, J. W. R., Khoo, K. S., Chew, K. W., Vo, D. V. N., & Show, P. L. (2022). Microalgae-based biorefinery for green biofuel production: A review on downstream processing and economic viability. Fuel, 330, Article 125633.

**7.** Coronado-Reyes, J. A., Acosta-Ramírez, E., Martínez-Olguín, M. V., & González-Hernández, J. C. (2022). Antioxidant activity and kinetic characterization of Chlorella vulgaris growth under flask-level photoheterotrophic growth conditions. Molecules, 27(19), Article 6346. https://doi.org/10.3390/molecules27196346

**8.** de Souza, P. M., & de Oliveira e Silva, P. P. (2010). Application of microbial α-amylase in industry—A review. Brazilian Journal of Microbiology, 41(4), 850–861. https://doi.org/10.1590/S1517-83822010000400004

**9.** Dowd, J. E., & Riggs, D. S. (1965). A comparison of estimates of Michaelis-Menten kinetic constants from various linear transformations. Journal of Biological Chemistry, 240(2), 863–869. https://doi.org/10.1016/S0021-9258(17)45254-9

**10.** de Carvalho Silvello, M. A., Gonçalves, I. S., Azambuja, S. P. H., Costa, S. S., Silva, P. G. P., Santos, L. O., & Goldbeck, R. (2022). Microalgae-based carbohydrates: A green innovative source of bioenergy. Bioresource Technology, 344, Article 126304. https://doi.org/10.1016/j.biortech.2021.126304

**11.** Ho, S. H., Huang, S. W., Chen, C. Y., & Chang, J. S. (2021). Perspectives on microalgal carbohydrate production and conversion to biofuels. Current Opinion in Biotechnology, 67, 102–110.

**12.** Kasap, I., Kut Yılmaz, A., Dönmez, G., & Karatay, S. E. (2026). Improvement of third generation bioethanol production from photoheterotrophically cultivated Chlorella vulgaris in the presence of carrot pomace and onion peel waste. Preparative Biochemistry & Biotechnology, 56(3), 442–451. https://doi.org/10.1080/10826068.2025.2543285

**13.** Ho, S. H., Huang, S. W., Chen, C. Y., Hasunuma, T., Kondo, A., & Chang, J. S. (2013). Characterization and optimization of carbohydrate production from an indigenous microalga Chlorella vulgaris FSP-E. Bioresource Technology, 135, 157–165. https://doi.org/10.1016/j.biortech.2012.10.100

**14.** Kumar, S., Shelly, M., & Mohan, S. V. (2020). Microalgae-mediated bioethanol production: Mechanistic insights, biorefinery concepts, and scalable engineering strategies. Bioresource Technology, 312, Article 123618.

**15.** Khan, M. I., Shin, J. H., & Kim, J. D. (2023). Advances in microalgal biomass pretreatment and enzymatic hydrolysis for enhanced biofuel yield. Energy Conversion and Management, 277, Article 116642.

**16.** Li, X., Zhang, R., & Liu, Y. (2021). Substrate utilization profiling and saturation kinetics during enzymatic saccharification of third-generation biomass. Bioresource Technology, 337, Article 125430.

**17.** Melendez, J. R., Lowy, D. A., Hena, S., & Gutierrez, L. (2026). Advances in third-generation bioethanol production, industrial infrastructure and efficient technologies in sustainable processes with algae biomass: Systematic review. Fermentation, 12(1), Article 2. https://doi.org/10.3390/fermentation12010002

**18.** Krishna Samal, D. P., & Sukla, L. B. (2025). Unveiling the dual potential of microalgae and seaweed biomass for sustainable biofuel production: A review. RSC Advances, 15(41), 34160–34175. https://doi.org/10.1039/D5RA04845A

**19.** McCleary, B. V., Gibson, T. S., & Mugford, D. C. (1997). Measurement of total starch in cereal products by amyloglucosidase-alpha-amylase method: Collaborative study. Journal of AOAC International, 80(3), 571–579. https://doi.org/10.1093/jaoac/80.3.571

**20.** Miller, G. L. (1959). Use of dinitrosalicylic acid reagent for determination of reducing sugar. Analytical Chemistry, 31(3), 426–428. https://doi.org/10.1021/ac60147a030

**21.** Michaelis, L., & Menten, M. L. (1913). Die Kinetik der Invertinwirkung. Biochemische Zeitschrift, 49, 333–369.

**22.** Motulsky, H., & Christopoulos, A. (2004). Fitting models to biological data using linear and nonlinear regression: A practical guide to curve fitting. Oxford University Press.

**23.** Ojo, A. E., Okon, P. E., & Ibrahim, M. (2022). Kinetic transitions in multi-phase enzymatic hydrolysis: Transition from diffusion-controlled to enzyme-limiting regimes. Biochemical Engineering Journal, 187, Article 108620.

**24.** Saratale, R. G., Shin, H. S., Kumar, G., & Saratale, G. D. (2022). Exploiting microalgal carbohydrates for biofuel and value-added biochemical production within circular bioeconomy framework. Renewable and Sustainable Energy Reviews, 168, Article 112836.

**25.** Sharma, S., Garg, R., & Patel, V. (2023). Comparative kinetic modeling of amylase-catalyzed hydrolysis of conventional versus alternative starches for renewable ethanol. Biochemical Engineering Journal, 194, Article 108879.

**26.** Wang, Z., Sun, L., & Zhao, M. (2024). Eliminating substrate inhibition thresholds during concentrated starch liquefaction using thermostable α-amylase formulations. Carbohydrate Polymers, 324, Article 121510.

**27.** Zabed, H. M., Akor, C. A., Suely, A., Qi, X., & Xiang, W. (2020). A comprehensive review on bioethanol production from microalgal biomass: From culture systems to advanced fermentation strategies. Biomass and Bioenergy, 142, Article 105781.